Intrinsic magnetism in penta-hexa-graphene: A first-principles study

Yierpan Aierken,[*] Ortwin Leenaerts,[†] and François M. Peeters[‡]
Department of Physics, University of Antwerp, Groenenborgerlaan 171, 2020 Antwerpen, Belgium
(Received 7 July 2016; revised manuscript received 1 September 2016; published 10 October 2016)

Recently, several monolayer carbon allotropes have been proposed. The magnetic properties of these metal-free materials are investigated, and we explore a special type of all carbon system having an intrinsic magnetic ground state. The structure is composed of mixing pentagonal and hexagonal rings of carbon atoms, such that the unit cell consists of eleven atoms, where two C atoms each have an unpaired electron each with a local magnetic moment. The antiferromagnetic (AFM) state has a lower energy than the ferromagnetic (FM) one. However, a strain-driven transition to the FM ground state is possible. The application of strain not only lowers the energy of the FM state but it also induces an energy barrier of about 13 meV/(magnetic atom) to protect the FM state from excitation. Our findings based on first-principles calculations will motivate other works on similar metal-free magnetic monolayer materials and will have an impact on their possible applications in spintronic devices.

DOI: 10.1103/PhysRevB.94.155410

I. INTRODUCTION

More and more two-dimensional (2D) crystal materials with distinct properties are predicted and synthesized. Especially, graphene [1,2] and its derivatives [3,4] are under intensive research to either modify their known properties or to increase their functionality. Considering the very low spin-orbit coupling and long spin relaxation time in these systems, substantial effort has been devoted to the induction of magnetism in these metal-free materials with the aim for future spintronic devices [5,6]. Intrinsic magnetism in graphene is absent, but extrinsic magnetism has been achieved by means of partial hydrogenation [7,8], foreign atom substitution [9,10], and the introduction of defects [11,12].

Three types of orbital hybridization are usually found in carbon allotropes, namely sp, sp^2, and sp^3. While graphene is made of a network of sp^2 hybridized atoms connected through σ and π bonds of p_z orbitals, diamond is exclusively held together by σ bonds between sp^3 bonded atoms. Another class of carbon allotropes is formed by the graphynes and graphdiynes [13,14]. These flat materials contain a mixture of sp and sp^2 hybridized C atoms. Structures containing a mixture of sp^2 and sp^3 atoms, such as penta-graphene [15], have been studied [16–18] as well. This last structure contains a mixture of threefold and fourfold coordinated C atoms. This leads to a distorted structure with nonideal bond angles that has higher formation energy than the nondistorted graphene and diamond crystals with their ideal planar and tetrahedral bonding geometry. Therefore, a system with a local bond structure resembling that of graphene or diamond will have lower energy.

None of the above mentioned materials are magnetic because they contain only paired electrons. Local magnetic moments usually originate from lone electrons that are not involved in chemical bonding. Single atomic defects such as vacancies break covalent bonds and create lone electrons that give rise to magnetism. It is interesting to investigate whether a structural modification with a proper mixing of three- and fourfold coordinated C atoms can lead to local magnetic moments in a stable crystalline structure. In this paper we propose such a type of 2D carbon allotrope with nontrivial magnetic properties. This structure is composed of a mixture of pentagonal and hexagonal rings of carbon atoms and will be called penta-hexa-graphene (ph-graphene). This material has an antiferromagnetic (AFM) ground state which transforms to a ferromagnetic (FM) state under strain. The latter state is protected by a small strain-induced energy barrier. These findings can initiate further research to induce magnetism and spin-flip barriers through strain in other metal-free 2D materials.

Recently, Zhang *et al.* [19] reported our proposed structure in their supplementary materials. These authors discussed the possibilities of the experimental realization of this type of structure from C_{36} quasi-2D membranes. However, a detailed study of the physical properties, especially the magnetic properties, of our proposed structure was not reported. The effect of strain on the magnetic properties was also not investigated in Ref. [19].

II. COMPUTATIONAL DETAILS

Our first-principles calculations are based on spin-polarized density functional theory as implemented in the Vienna *ab initio* simulation package (VASP) [20]. The cutoff energy for the plane-wave basis used to expand the wave functions is set to 500 eV. This is large enough to guarantee the convergence of the relative energy differences between different ground states. The projected augmented wave (PAW) method [21] is used to describe the wave functions. Exchange-correlation interactions are described with the generalized gradient approximation (GGA) within the Perdew-Burke-Ernzerhof (PBE) formulation [22,23]. The Brillouin-zone sampling is done with a $15 \times 15 \times 1$ k-points mesh for monolayer structures. A vacuum space of 25 Å is included to simulate a monolayer environment. The self-consistency convergence criterion for the total energy is set to 10^{-8} eV. The ionic optimization criterion for the atomic forces is set to 10^{-7} eV/Å. These high criteria are required to perform accurate phonon calculations.

[*]yierpan.aierken@uantwerpen.be
[†]ortwin.leenaerts@uantwerpen.be
[‡]francois.peeters@uantwerpen.be

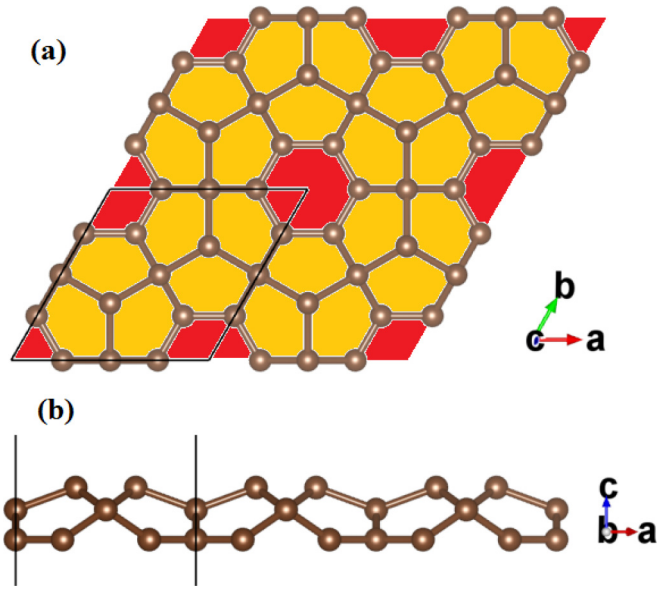

FIG. 1. Atomic structure of a 2 × 2 supercell of monolayer ph-graphene. (a) Top view with hexagonal and pentagonal rings marked with red and yellow color, respectively; (b) Side view of the buckled structure (visualisation using VESTA [25]).

These phonon calculations are done in a 3 × 3 × 1 supercell with the Phonopy code [24].

III. STRUCTURAL, ELECTRONIC PROPERTIES, AND STABILITY

The structure of the proposed 2D material is schematically shown in Fig. 1. It consists of hexagonal rings of C atoms surrounded by six pentagonal rings which share one edge with the hexagon and four with other pentagons. These hexagonal and pentagonal rings are arranged in a hexagonal lattice to form an infinite monolayer sheet. Considering the complex structure of this system, it is important to understand the hybridization of the electronic orbitals. For this, we calculate the hybridization index of the three C atoms that have a unique local environment, namely C1, C2, and C3 in Fig. 2, through Coulson's theorem: $1 + \sqrt{n_1 n_2} cos\theta_{12} = 0$, where θ_{12} is the interorbital angle between orbital 1 and 2 (see Fig. 2) and n is the hybridization index. n corresponds to the index in the sp^n notation and determines the relative fraction of p orbitals with respect to the s orbital. The sum of the s fractions in all hybridized orbitals should equal 1, while it should be 3 for the sum of the p fractions.

TABLE I. Orbital hybridization indices of the C atoms in ph-graphene.

Atom	Orbitals			
	φ_1	φ_2	φ_3	φ_4
C1	2.00	2.00	2.72	14.58
C3	3.11	3.11	3.11	2.70

In Table I, we list the hybridization indices n of the C1 and C3 orbitals which are denoted as φ_i, where i is the index for different orbitals. The C1 atom has two sp^2 orbitals with 120° interorbital angle and one $sp^{2.72}$. The latter gives rise to a partly buckled structure. The fourth C1 orbital has a large p contribution, indicating that it is close to a p_z orbital with little s contribution, and induces π bonding in the hexagonal rings. The C2 atoms have fourfold coordination and their hybridization should be close to sp^3. Due to geometric constraints, the bonds have strained angles [26]. Finally, the C3 atom has four quasi-sp^3 orbitals of which three are used for nearest-neighbor σ bonding. The electron in the fourth orbital remains unpaired and can give a local magnetic moment of 1 μ_B (Bohr magneton). There are two C3 atoms per unit cell which form a graphenelike subcrystal. The maximal magnetic moment per unit cell is therefore 2 μ_B if the system is ferromagnetic. However, when we align these two magnetic moments antiparallel, the total energy is lowered by 12 meV per magnetic atom, which gives an AFM ground state.

In comparison to penta-graphene, ph-graphene has a 76 mev/atom lower formation energy. However, it is about 0.9 eV/atom higher than that of graphene. These results are consistent with the ones from Zhang *et al.* [19]. The relatively high formation energy of ph-graphene as compared

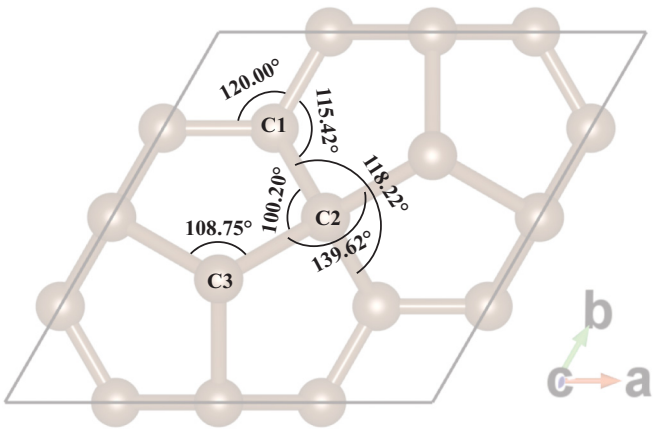

FIG. 2. Bond angles in the unit cell of monolayer ph-graphene.

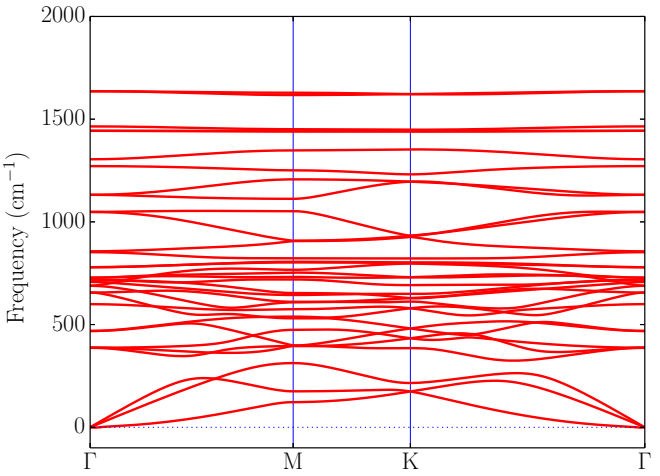

FIG. 3. Phonon dispersion relation of monolayer ph-graphene.

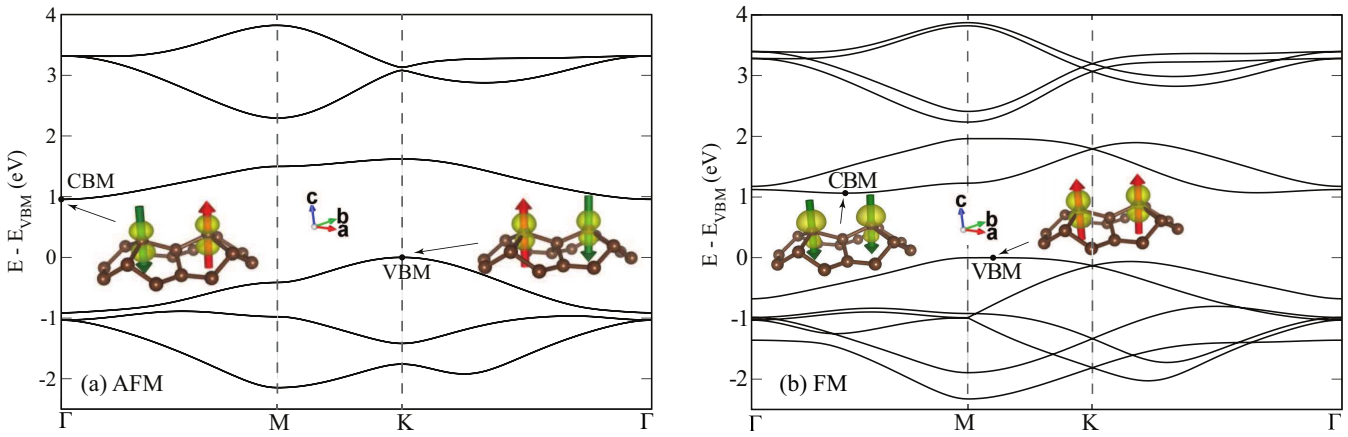

FIG. 4. Electronic band structure of monolayer ph-graphene of the (a) AFM and the (b) FM state. The charge densities at the VBM and CBM in the unit cell are shown as insets. The arrows on the atoms indicate the orientation of their magnetic moments.

to graphene can be mainly attributed to the "bent" bonds of the C2 atoms due to geometric constraints.

To check the dynamical stability of the ph-graphene structure, we calculated its phonon spectrum (see Fig. 3). Since there are no imaginary frequencies, we can conclude that the structure is dynamically stable.

The electronic band structure and the charge densities at the valence band maximum (VBM) and conduction band minimum (CBM) are shown in Fig. 4. Both the FM and AFM states exhibit indirect semiconducting character with a band gap (PBE) of 1.06 eV and 0.96 eV, respectively. The band edge states are mainly located on the magnetic atoms and the band gap separates states of opposite spin orientation. The hybridized φ_4 states (see above) on these atoms form a π bonding network that resembles the p_z π bonding in graphene. For the FM state, the typical graphenelike band structure that results from this can be observed for the valence and conduction bands. These bands are separated due to the ferromagnetic exchange splitting in spin-up and spin-down states with a large gap in between. Note that the splitting between bonding and antibonding states at the Γ point is strongly reduced with respect to graphene because of the larger interatomic distance separating the C3 atoms (3.1 Å in ph-graphene vs 1.4 Å in graphene). Due to this increased bonding distance, the exchange interaction exceeds the bonding interaction and the system is magnetic in stark contrast to graphene where the π bonding is much stronger.

IV. EFFECT OF STRAIN: AFM-FM TRANSITION

Strain is an effective way to modulate the electronic properties of materials. There are different ways to induce strain in 2D materials. Roldán *et al.* [27] have given a comprehensive review on strain engineering of 2D materials, both from experimental and theoretical views. Here, we apply biaxial strain to our structure and monitor how the total energy of the different magnetic phases change, see Fig. 5. We find that an AFM to FM transition occurs for both compressive and tensile strains of approximately 6% and 8%, respectively. Therefore, strained structures of this kind can give an FM ground state, which is more beneficial for applications. The variation of the band gap under strain is plotted in Fig. 6. Both the FM and the AFM band gap has a similar qualitative behavior with a small quantitative difference between the

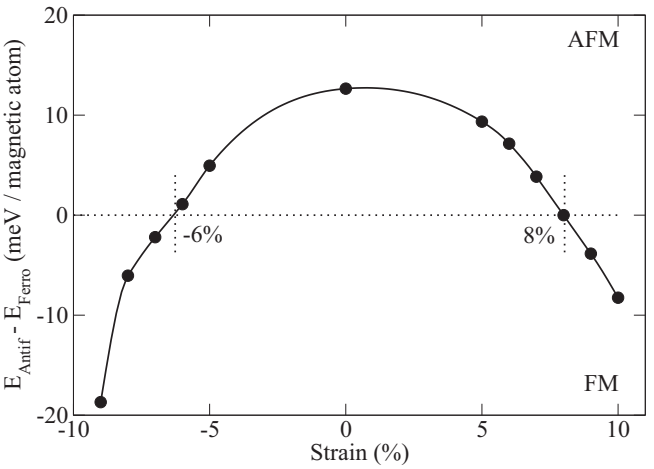

FIG. 5. The transition of monolayer ph-graphene between the AFM and the FM state under strain.

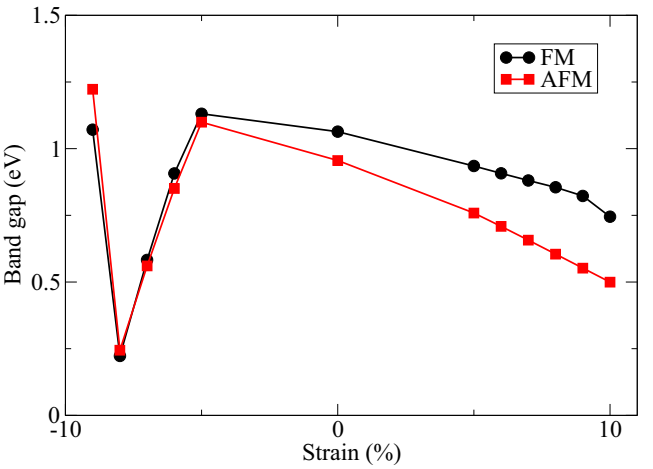

FIG. 6. Band gap variation of AFM and FM monolayer ph-graphene under strain.

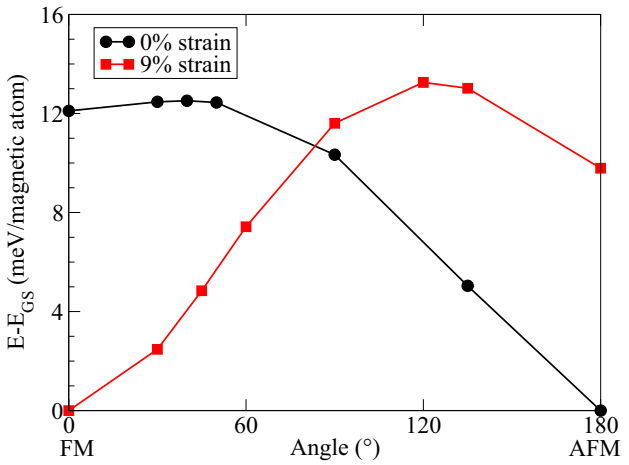

FIG. 7. AFM to FM transition through spin-flip in monolayer ph-graphene.

two magnetic phases. Tensile strain decreases the band gap monotonically up to 10%, while compressive strain gives a nonmonotonic behavior due to band crossings. From −5% to 10% strain, CBM and VBM are located at the Γ and K high symmetric k points, respectively, while two transitions of the location of the VBM happen below −5% strain. First, it is shifted to the Γ k point from the second highest valence band around −8% and then shifted to the Σ k path between the Γ and M k points at −9%.

As a final property of the two different magnetic ground states, we study the energy barrier for the transition from the FM to AFM state through spin flipping. This calculation is realized by constraining the magnetic moment through a penalty contribution to the total energy in VASP, and rotating one of the moments stepwise through 180°. In this way an energy profile from FM to AFM can be obtained (see Fig. 7). The rotation of the magnetic moment was carried out along two different planes, one along the zigzag direction and the other along the armchair direction, but the difference in the energy profile is negligible.

Without strain, there is almost no energy barrier for the transition from the FM to AFM state. However, if the structure is under a 9% tensile strain, in which case the FM state is the ground state, an energy barrier of about 13 meV per magnetic atom has to be overcome to reach the AFM state. This is much larger than the energy barrier from the AFM to the FM under the same strain, which is about 3.3 meV per magnetic atom. This calculation informs us about the stability of each magnetic state and the possibility to form a paramagnetic state. We found that both magnetic states are stable and that there is no tendency to form a noncollinear magnetic moment orientation.

V. SUMMARY AND CONCLUSIONS

In this paper, we proposed a type of stable monolayer carbon allotrope composed of pentagonal and hexagonal rings of carbon atoms. We explained the symmetry and the structure of the bonds that result in local magnetic moments. By comparing the total energy of the FM and AFM state, we conclude that the latter is the ground state.

We discovered a strain-driven magnetic ground state transition from AFM to FM around 6% compressive strain and 8% tensile strain. The energy as a function of angle between two local magnetic moments is calculated to study the energy barrier for the transition between FM and AFM. While an energy barrier of about 13 meV/(magnetic atom) was found that protects the AFM ground state in the pristine case; it is protecting the FM ground state when the system is under 9% tensile strain. Our theoretical calculations give insight into the magnetic mechanism in this metal-free material, which can initiate further work on the exploration of the magnetic properties of other 2D metal-free material.

ACKNOWLEDGMENTS

This work was supported by the Fonds Wetenschappelijk Onderzoek (FWO-Vl). The computational resources and services used in this work were provided by the VSC (Flemish Supercomputer Center), funded by the Research Foundation-Flanders (FWO) and the Flemish Government-department EWI.

[1] K. S. Novoselov, A. K. Geim, S. V. Morozov, D. Jiang, Y. Zhang, S. V. Dubonos, I. V. Grigorieva, and A. A. Firsov, Science **306**, 666 (2004).
[2] A. K. Geim and K. S. Novoselov, Nat. Mater. **6**, 183 (2007).
[3] V. Georgakilas, M. Otyepka, A. B. Bourlinos, V. Chandra, N. Kim, K. C. Kemp, P. Hobza, R. Zboril, and K. S. Kim, Chem. Rev. **112**, 6156 (2012).
[4] M. Inagaki and F. Kang, J. Mater. Chem. A **2**, 13193 (2014).
[5] E. Kan, Z. Li, and J. Yang, Nano **03**, 433 (2008).
[6] K. Xu, X. Li, P. Chen, D. Zhou, C. Wu, Y. Guo, L. Zhang, J. Zhao, X. Wu, and Y. Xie, Chem. Sci. **6**, 283 (2015).
[7] J. Zhou, Q. Wang, Q. Sun, X. S. Chen, Y. Kawazoe, and P. Jena, Nano Lett. **9**, 3867 (2009).
[8] A. Y. S. Eng, H. L. Poh, F. Šaněk, M. Maryško, S. Matějková, Z. Sofer, and M. Pumera, ACS Nano **7**, 5930 (2013).
[9] S. Okada and A. Oshiyama, Phys. Rev. Lett. **87**, 146803 (2001).
[10] Q. Miao, L. Wang, Z. Liu, B. Wei, F. Xu, and W. Fei, Sci. Rep. **6**, 21832 (2016).
[11] V. M. Pereira, F. Guinea, J. M. B. Lopes dos Santos, N. M. R. Peres, and A. H. Castro Neto, Phys. Rev. Lett. **96**, 036801 (2006).
[12] O. V. Yazyev and L. Helm, Phys. Rev. B **75**, 125408 (2007).
[13] R. H. Baughman, H. Eckhardt, and M. Kertesz, J. Chem. Phys. **87**, 6687 (1987).
[14] A. Ivanovskii, Prog. Solid State Chem. **41**, 1 (2013).
[15] S. Zhang, J. Zhou, Q. Wang, X. Chen, Y. Kawazoe, and P. Jena, PNAS **112**, 2372 (2015).
[16] F. Q. Wang, J. Yu, Q. Wang, Y. Kawazoe, and P. Jena, Carbon **105**, 424 (2016).
[17] Z. G. Yu and Y.-W. Zhang, J. Appl. Phys. **118**, 165706 (2015).

[18] G. R. Berdiyorov and M. E.-A. Madjet, RSC Adv. **6**, 50867 (2016).
[19] X. Zhang, L. Wei, J. Tan, and M. Zhao, Carbon N. Y. **105**, 323 (2016).
[20] G. Kresse and J. Hafner, Phys. Rev. B **49**, 14251 (1994); G. Kresse and J. Furthmüller, Comput. Mater. Sci. **6**, 15 (1996); Phys. Rev. B **54**, 11169 (1996); G. Kresse and J. Hafner, *ibid.* **47**, 558 (1993).
[21] P. E. Blöchl, Phys. Rev. B **50**, 17953 (1994); G. Kresse and D. Joubert, *ibid.* **59**, 1758 (1999).
[22] J. P. Perdew, K. Burke, and M. Ernzerhof, Phys. Rev. Lett. **77**, 3865 (1996).
[23] J. P. Perdew, K. Burke, and M. Ernzerhof, Phys. Rev. Lett. **78**, 1396 (1997).
[24] A. Togo and I. Tanaka, Scr. Mater. **108**, 1 (2015).
[25] K. Momma and F. Izumi, J. Appl. Crystallogr. **44**, 1272 (2011).
[26] C. Coulson and W. Moffitt, Phil. Mag. **40**, 1 (1949).
[27] R. Roldán, A. Castellanos-Gomez, E. Cappelluti, and F. Guinea, J. Phys.: Condens. Matter **27**, 313201 (2015).